Drosophila pVALIUM10 TRiP RNAi lines cause undesired silencing of Gateway-based transgenes

Dimitrije Stanković[1], Gábor Csordás[2], Mirka Uhlirova[1#]

[1]Institute for Genetics and Cologne Excellence Cluster on Cellular Stress Responses in Aging-Associated Diseases (CECAD), University of Cologne, Cologne, Germany

[2]Institute of Genetics, Biological Research Centre of the Eötvös Loránd Research Network, Szeged, Hungary

[#] Address correspondence to Mirka Uhlirova, mirka.uhlirova@uni-koeln.de

Running title: pVALIUM10 TRiP lines silence Gateway-based transgenes

Keywords: *Drosophila*, RNAi, dsRNA, pValium10, Gateway recombination, TRiP lines

SUMMARY

Post-transcriptional gene silencing using double-stranded RNA has revolutionized the field of functional genetics, allowing fast and easy disruption of gene function in various organisms. In *Drosophila*, many transgenic RNAi lines have been generated in large-scale efforts, including the *Drosophila* Transgenic RNAi Project (TRiP), to facilitate *in vivo* knockdown of virtually any *Drosophila* gene with spatial and temporal resolution. The available transgenic RNAi lines represent a fundamental resource for the fly community, providing an unprecedented opportunity to address a vast range of biological questions relevant to basic and biomedical research fields. However, caution should be applied regarding the efficiency and specificity of the RNAi approach. Here, we demonstrate that pVALIUM10-based RNAi lines, representing ~13% of the total TRiP collection (1,808 out of 13,410 TRiP pVALIUM-based RNAi lines), cause unintended off-target silencing of transgenes expressed from Gateway destination vectors generated via site-specific recombination. The silencing is mediated by targeting attB1 and attB2 sequences generated in the recombination reaction and included in the transcribed mRNA. Deleting these attB sites from the Gateway expression vector prevents silencing and restores expected transgene expression.

INTRODUCTION

Double-stranded RNA (dsRNA)-mediated post-transcriptional gene silencing, also known as RNA interference (RNAi), represents an ancient anti-viral defense mechanism that has been harnessed as a powerful tool for reverse functional genetics in various cultured cells, plant and animal model systems (Kennerdell & Carthew, 1998; Lohmann *et al*, 1999; Wargelius *et al*, 1999; Wianny & Zernicka-Goetz, 2000; Zamore *et al*, 2000). The dsRNA silencing relies on a highly conserved RNase III enzyme called Dicer that recognizes and processes dsRNA into small 21-23-bp segments (siRNA). Upon loading into a multiprotein RNA-induced silencing complex (RISC), the guide strand facilitates pairing with complementary on-target

41 RNAs, which are subsequently degraded by the action of the Argonaut proteins (Tomari & Zamore, 2005).
42 In *Drosophila*, spatio-temporally controlled RNAi knockdown can be achieved by expressing dsRNA using
43 transgenic binary expression systems, such as Gal4/UAS (Brand & Perrimon, 1993). The initial transgenic
44 RNAi lines were generated using plasmids with ligated inverted repeats transcribed from one (Kennerdell
45 & Carthew, 1998) or two opposite promoters (Giordano *et al*, 2002). However, these vectors were
46 unstable and not well tolerated by the bacterial strains commonly used for cloning (Hagan & Warren,
47 1983; Piccin *et al*, 2001), a problem later solved by the introduction of an intron spacer between the
48 repeats (Bao & Cagan, 2006; Lee & Carthew, 2003). This step-by-step progress led to the development of
49 the pVALIUM (Vermilion-attB-LoxP-Intron-UAS-MCS), a universal vector system for transgenic RNAi library
50 generation. The pVALIUM RNAi vectors contain an eye-color selection marker (*vermillion*), an attB site
51 enabling phiC31-mediated site-directed integration into predefined genomic locations, *white* or *ftz*
52 introns promoting the processing of dsRNA, and a cassette of two UAS pentamers, one of which is flanked
53 by loxP sites to allow tuning of the dsRNA expression levels, as well as a multiple cloning site (MCS) (Ni *et*
54 *al*, 2008).
55 The highly efficient pVALIUM10-based transgenic RNAi stocks produced within the *Drosophila* Transgenic
56 RNAi Project (TRiP) at Harvard Medical School (HMS) (https://fgr.hms.harvard.edu) represent an
57 invaluable resource for the *Drosophila* community (Perkins *et al*, 2015). At the moment of writing, 1,808
58 transgenic TRiP RNAi stocks based on the pVALIUM10 are available at the Bloomington *Drosophila* stock
59 center (BDSC, https://bdsc.indiana.edu/index.html) (Perrimon *et al*, 2010). The pVALIUM10 vector carries
60 *gypsy* insulators that markedly enhance knockdown efficiency, along with two inverted "attR1-selection-
61 attR2" cassettes that facilitate cloning of dsRNA fragments via site-specific Gateway *in vitro*
62 recombineering (Ni *et al*, 2009; Reece-Hoyes & Walhout, 2018). A desired single fragment, 400 - 600 bp
63 in length and flanked by attL1 and attL2 recombination sites, can be easily moved from an entry vector

64 into a pVALIUM10 destination vector via recombination between attL and attR sites catalyzed by LR
65 clonase, producing a vector for UAS-driven expression of dsRNA (Ni *et al.*, 2009).
66 The Gateway cloning technology is also routinely used to generate transgenic constructs for expression of
67 epitope-tagged or untagged proteins, taking advantage of the *Drosophila* Gateway™ plasmid collection at
68 the *Drosophila* Genomics Resource Center (https://dgrc.bio.indiana.edu/). Importantly, as with
69 pVALIUM10 dsRNA plasmids, production of Gateway expression vectors relies on the recombination
70 between attL and attR sites resulting in the formation of attB1 and attB2 sites.
71 Here, we demonstrate that the pVALIUM10-derived RNAi lines cause undesirable knockdown of
72 transgenic reporters and overexpression lines generated with the help of the Gateway cloning technology.
73 They do so by targeting the attB sites that are part of the transcribed mRNA. Deletion of the attB1 and
74 attB2 sequences from the Gateway expression destination vector abrogates this effect and restores
75 expected transgene expression levels.
76
77
78 **RESULTS**
79 **Unexpected, off-target silencing of the RNAse H1::GFP reporter by multiple pVALIUM10-RNAi lines**
80 *In vivo* RNAi-based genetic screens have proved very successful in identifying novel genes involved in
81 developmental and pathologic processes in a variety of *Drosophila* somatic tissues when expressed using
82 tissue-specific Gal4 driver lines (Graca *et al*, 2021; Lesch *et al*, 2010; Neely *et al*, 2010; Pletcher *et al*, 2019;
83 Port *et al*, 2011; Rotelli *et al*, 2019; Rylee *et al*, 2022; Saj *et al*, 2010; Zeng *et al*, 2015; Zhou *et al*, 2019).
84 Hence, we embarked on a candidate genetic screen aimed at identifying factors controlling genome
85 stability. During the pre-screening of potential candidates we observed that expression of pVALIUM10-
86 based *BuGZ*$^{RNAi[TRiP.JF02830]}$ RNAi line in the pouch region of the developing third instar wing discs, using the
87 *nubbin-Gal4, UAS-mRFP* (*nub>mRFP*) driver line, efficiently suppressed the multi-epitope tagged BuGZ

88 transgene (*BuGZ*$^{FlyFos[v318366]}$) (Sarov *et al*, 2006) (Figure 1A, B, D). A similar reduction was observed using
89 an independent *BuGZ*$^{RNAi[KK104498]}$ line from the Vienna *Drosophila* Resource Center (VDRC) KK RNAi library
90 (Figure 1C, D). Encouraged by these results, both BuGZ RNAi lines were included in the candidate genetic
91 screen that was based on expression of selected dsRNAs with the *nub>mRFP* driver. As readout for
92 genome stability, we used the ubiquitously driven RNase H1::GFP that was generated by recombining the
93 *RNase H1* coding sequence into the pUWG vector from the *Drosophila* Gateway™ plasmid collection. This
94 resulted in the expression of a C-terminally GFP-tagged RNase H1 under the control of the poly-ubiquitin
95 promoter (Figure 2A, B). The RNase H1 enzyme recognizes and resolves R-loops, DNA:RNA hybrids, that
96 emerge during transcription and represent a threat to genome stability when unresolved (Crossley *et al*,
97 2019; Santos-Pereira & Aguilera, 2015). Unexpectedly, we observed reduction of RNase H1::GFP signal
98 when expressing *BuGZ*$^{RNAi[TRiP.JF02830]}$ but not *BuGZ*$^{RNAi[KK104498]}$ line (Figure 2C, D, H). Strikingly, similar
99 downregulation of RNase H1::GFP was caused by pVALIUM10-based *myc*$^{RNAi[TRiP.JF01761]}$ but not
100 *myc*$^{RNAi[TRiP.HMS01538]}$ or *myc*$^{RNAi[GD2948]}$ derived from pVALIUM20 and pMF3 vectors, respectively (Figures 1D
101 and 2E-H). All three myc-RNAi lines have been shown effective by others (Aughey *et al*, 2016; Kim-Yip &
102 Nystul, 2018; Ledru *et al*, 2022; Rust *et al*, 2018). These results indicated that the tested pVALIUM10 TRiP
103 RNAi lines but not pVALIUM20, KK or GD lines may cause undesirable silencing of the RNase H1::GFP
104 transgene. We further speculated that dsRNA expressed from pVALIUM10 contains segments unrelated
105 to the target gene-specific sequences that trigger this unexpected off-target effect.
106
107 **pVALIUM10 RNAi and Gateway expression plasmids share attB recombination sites**
108 To identify the potential target for dsRNA-mediated knockdown of the RNAse H1::GFP transgene by
109 pVALIUM10 TRiP RNAi, we compared the plasmid sequences. We found that attB1 and attB2 sites are
110 shared between the Gateway-based expression vectors, including pUWG, and pVALIUM10 TRiP RNAi
111 plasmids. AttB1 and attB2 sites are 25 bp in length and generated by LR clonase-mediated recombination

112 between attL and attR sequences. Given the repetition of attB1 and attB2 sites, flanking the passenger
113 and guide target sequence fragments in pVALIUM10 TRiP RNAis, these sequences are transcribed and
114 could contribute to the dsRNA stem-loop substrate for Dicer. Based on these results we hypothesized that
115 dsRNAs generated from attB1 and attB2 could target, and thus silence, Gateway-based transgenes via
116 attB sites (Figure 2I).
117

118 **pVALIUM10 RNAi lines silence Gateway transgenes via attB sites**

119 To test our hypothesis, we cloned the *mCherry* coding sequence into the pUWG Gateway expression
120 vector (pUWG-*mCherry*) allowing ubiquitous expression of mCherry transcript flanked by the attB1 and
121 attB2 sites. The pUWG-*mCherry* vector then served as a template for overlap PCR to generate the
122 pUWG$^{\Delta attB}$-*mCherry* construct that lacks attB sites (Figure 3A). Both plasmids were used to establish
123 transgenic fly lines through a standard *Drosophila* germline transformation method (Rubin & Spradling,
124 1982). The susceptibility or resistance of *ubi-mCherry* (pUWG-*mCherry*) and *ubi$^{\Delta attB}$-mCherry* (pUWG$^{\Delta attB}$-
125 *mCherry*) transcripts to RNAi-mediated silencing was then tested by driving various RNAi lines under the
126 control of the *nub-Gal4* driver. Immunostaining of the third instar wing imaginal discs using an anti-RFP
127 antibody revealed an identical pattern of ubi-mCherry and ubi$^{\Delta attB}$-mCherry transgenes in the control
128 (*nub>*) background (Figure 3B, C). In contrast, levels of ubi-mCherry but not ubi$^{\Delta attB}$-mCherry transgenic
129 protein were markedly reduced in the wing pouch region relative to the rest of the tissue following
130 overexpression of *BuGZ* and *myc* pVALIUM10 TRiP RNAi lines (Figure 3D, E, H, I, J, M) while no significant
131 changes were observed when *BuGZ* and *myc* were knocked down using KK and pVALIUM20 RNAi lines,
132 respectively (Figure 3F, G, H, K, L, M). Importantly, the attB site-dependent silencing of ubi-mCherry was
133 recapitulated using an additional set of pVALIUM10 TRiP RNAi lines targeting *Atf3*, *Lip4*, *yki*, *DH44*, *ftz-f1*,
134 *mago*, *brat*, and *Actβ* genes (Supplementary Figure S1).

135 Finally, we tested whether pVALIUM10 TRiP RNAi lines may also interfere with UAS-inducible attB-
136 containing transcripts, such as transgenic fly open reading frames (ORFs) expressed from the Gateway
137 destination vector pGW-HA.attB (Bischof *et al*, 2014). To this end, we assessed levels of the HA-tagged
138 SmD3 FlyORF protein in the presence of pVALIUM10 or KK BuGZ-RNAi line. In contrast to an enrichment
139 of SmD3::3xHA protein and positive punctae in the wing pouch cells of control (*nub>*) and *BuGZ*$^{RNAi[KK104498]}$
140 expressing wing discs, the overall levels and the number of positive punctae were noticeably reduced in
141 *nub>BuGZ*$^{RNAi[TRiP.JF02830]}$ cells (Figure 3N-Q). These results suggest that the dsRNA hairpin produced from
142 pVALIUM10 RNAi vectors generates attB1- and attB2-siRNAs, which guide destruction of transcripts
143 containing such target sites. This off-target silencing via attB sites is specific to RNAi lines based on
144 pVALIUM10. Absence of attB1 and attB2 sites renders the Gateway-derived transcript resistant to
145 pVALIUM10 TRiP RNAi.
146
147
148 **DISCUSSION**
149 The use of transgenic RNAi to achieve developmental stage- and tissue-specific knockdown of candidate
150 genes and to perform genome-wide screens in *Drosophila* has become commonplace in the past two
151 decades (Blake *et al*, 2017; Dietzl *et al*, 2007; Hu *et al*, 2017; Port *et al.*, 2011). Both our knowledge on the
152 RNAi mechanism, and the tools to generate new types of RNAi constructs efficiently have considerably
153 evolved in recent years. As a result, several independent transgenic RNAi stock collections were
154 established, including Vienna *Drosophila* stock center (VDRC, 23,411 RNAi lines,
155 https://stockcenter.vdrc.at/control/main), Bloomington *Drosophila* Stock Center (BDSC, 13,698 RNAi
156 lines, https://bdsc.indiana.edu/), and the National Institute of Genetics (NIG, 12,365 RNAi lines,
157 https://shigen.nig.ac.jp/fly/nigfly/) at the time of writing. Yet, in spite of being a broadly used technique,
158 transgenic manipulation of gene expression can still have unforeseen consequences. A large portion of

159 the RNAi lines from the VDRC KK collection were found to produce phenotypes due to a secondary
160 insertion and consequent ectopic expression of the *tiptop* gene (Green *et al*, 2014; Vissers *et al*, 2016).
161 More recently, van der Graaf and colleagues reported that transgenes inserted in the commonly used
162 *attP40* landing site on the second chromosome can decrease the expression of Msp300, a member of the
163 LINC complex, and hence lead to nuclear size, shape and positioning phenotypes (van der Graaf *et al*,
164 2022).
165 Here, we demonstrate that the pVALIUM10-based RNAi lines cause off-target silencing of ORFs expressed
166 from Gateway expression vectors or potentially any transcripts containing attB1 and attB2 sites. We show
167 that the removal of these sites abrogates the undesirable knockdown. Given the popularity of the
168 Gateway expression vectors to generate transgenic protein-reporters and tagged overexpression
169 constructs, our results suggest that simultaneous use of pVALIUM10 TRiP RNAi may lead to experimental
170 artefacts unrelated to the investigated biological process.
171 Of note, in the original publication of pVALIUM10 vectors, the authors tested for potential off-target
172 effects by comparing the hairpin sequence against the *Drosophila* genome (Ni *et al.*, 2009), which does
173 not contain endogenous 21nt stretches equivalent to the attB1 and attB2 sequences. However, as the
174 transgenic toolkit in *Drosophila* is ever expanding, each additional transgene has the possibility to produce
175 a synthetic effect with the existing RNAi lines. Hence, we suggest that the researchers validate the type
176 of TRiP RNAi line or the expression vector sequence before commencing their experiments. As an
177 example, we do not recommend combining RNAi based on pVALIUM10 with the 3xHA-tagged
178 overexpression lines from FlyORF (https://flyorf.ch) (Bischof *et al.*, 2014) or the fly-FUCCI (Fluorescent
179 Ubiquitination-based Cell Cycle Indicator) lines, which allow real-time visualization of the cell cycle
180 dynamics by the expression two fluorescently tagged degrons (Zielke et al., 2014). In both cases, the
181 transgenes were generated via Gateway reaction and contains attB sites flanking the inserted ORF (Bischof
182 *et al.*, 2014; Zielke *et al*, 2014), which can lead to off-target silencing of the transcript. Furthermore, this

183 finding reinforces the idea that RNAi experiments should adhere to the standards established in the past
184 decades, including investigating possible off-target effects to eliminate knockdown of the unintended
185 gene, using multiple independent RNAi lines to recapitulate phenotypes, and confirming the knockdown
186 of the targeted gene products (Echeverri *et al*, 2006; Green *et al.*, 2014; Kaya-Çopur & Schnorrer, 2016).
187
188

189 **MATERIALS AND METHODS**

190 **Fly stocks and Husbandry**

191 The following *Drosophila* strains were used: w^{1118} (BDSC; RRID: BDSC_3605), *nubbin-Gal4, UAS-myr-mRFP*
192 (*nub>mRFP*), $BuGZ^{FlyFos[v318366]}$ (VDRC), $BuGZ^{RNAi[TRiP.JF02830]}$ (BDSC; RRID:BDSC_27996), $BuGZ^{RNAi[KK104498]}$
193 (VDRC), $Lip4^{RNAi[TRiP.HMO5136]}$ (BDSC; RRID:BDSC_28925), $myc^{RNAi[TRiP.JF01761]}$ (BDSC; RRID:BDSC_25783),
194 $myc^{RNAi[TRiP.HMS01538]}$ (BDSC; RRID:BDSC_36123), $myc^{RNAi[GD2948]}$ (VDRC), $Act\beta^{RNAi[TRiP.JF03276]}$ (BDSC;
195 RRID:BDSC_29597), $ftz\text{-}f1^{RNAi[TRiP.JF02738]}$ (BDSC; RRID:BDSC_27659), $yki^{RNAi[TRiP.JF03119]}$ (BDSC;
196 RRID:BDSC_31965), $Atf3^{RNAi[TRiP.JF02303]}$ (BDSC; RRID:BDSC_26741), $DH44^{RNAi[TRiP.JF01822]}$ (BDSC;
197 RRID:BDSC_25804), $brat^{RNAi[TRiP.HM05078]}$ (BDSC; RRID:BDSC_28590), $mago^{RNAi[TRiP.HM05142]}$ (BDSC;
198 RRID:BDSC_28931), $SmD3::3xHA^{[FlyORF\ F003987]}$ (FlyORF), $nub>SmD3::3xHA^{[FlyORF\ F003987]}$ (Erkelenz *et al*, 2021),
199 *ubi-RNase H1::GFP*, *ubi-mCherry*, $ubi^{\Delta attB}$*-mCherry* (this study). All *Drosophila* stocks are listed in
200 Supplementary Table S1. All crosses were set up and maintained at 25 °C, unless specified otherwise, on
201 a diet consisting of 0.8% agar, 8% cornmeal, 1% soymeal, 1.8% dry yeast, 8% malt extract, and 2.2% sugar-
202 beet syrup, which was supplemented with 0.625% propionic acid and 0.15% Nipagin. w^{1118} line was used
203 as control.
204

205 **Generation of plasmids and transgenic lines**

206 The open reading frame of *rnh1* (FBgn0023171) was amplified from *Drosophila melanogaster* cDNA (w^{1118})
207 using primers harboring NotI and SalI restriction sites. The stop codon was excluded to allow C-terminal
208 tagging of the protein. The ORF was cloned into the Gateway pENTR4 Dual Selection Vector (Thermo
209 Fisher Scientific; #A10465). The ORF was then recombined into the pUWG vector (DGRC; #1284) using the
210 LR Clonase II enzyme mix according to manufacturer's instructions (Thermo Fisher Scientific; #11791020).
211 The coding sequence of *mCherry* (GenBank: AY678264.1) was amplified with specific primers, cloned into
212 the pENTR 4 Dual Selection vector (Invitrogen, Cat. Nr. #A10465) including a stop codon and subsequently
213 recombined into the pUWG vector (pUWG-*mCherry*). Overlap PCR strategy was employed to generate the
214 pUWG$^{\Delta attB}$-*mCherry* construct lacking attB sites resulting from the LR recombination. Three separate PCR
215 reactions were performed to produce fragments for assembly using the original pUWG-*mCherry* plasmid
216 as a template. The forward primer of the first primer pair contained a XhoI restriction site, while the
217 reverse primer contained a XbaI restriction site. Partial complementarity of the reverse and forward
218 primers used to synthesize the downstream fragment enabled the exclusion of attB sites in the final
219 product. The final PCR product was ligated into the pUWG-*mCherry* plasmid digested with XbaI and XhoI.
220 Transgenic fly lines with random insertions of the constructs were generated by standard P-element-
221 mediated transformation using w^{1118} *Drosophila* strain. All primers and plasmids are listed in
222 Supplementary Table S2.
223
224 **Tissue dissection and immunostaining**
225 Wing imaginal discs dissected from third instar *Drosophila* larvae (7 days after egg laying (AEL)) were fixed
226 for 25 minutes with 4% paraformaldehyde in PBS containing 0.1% Triton X (PBS-T) at room temperature.
227 Fixed tissues were washed 3 times with PBS-T. Primary antibodies were diluted in blocking buffer (PBS-T
228 with 0.3% BSA) and tissues were stained overnight at 4 °C. The following primary antibodies were used:
229 rabbit anti-mRFP (1:500, MBL International Cat# PM005, RRID:AB_591279), goat anti-GFP (1:500, Abcam

230 Cat# ab6673, RRID:AB_305643), and rabbit-anti HA (1:1000, Abcam Cat# ab9110, RRID:AB_307019). After
231 washing, the samples were incubated with the corresponding Alexa Fluor 488 (1:2000, Thermo Fisher
232 Scientific Cat# A-11034, RRID:AB_2576217), Cy2 (1:2000, Jackson ImmunoResearch Labs Cat# 705-225-
233 147, RRID:AB_2307341) or Cy3 (Jackson ImmunoResearch Labs Cat# 711-165-152, RRID:AB_2307443)
234 conjugated secondary antibodies overnight at 4 °C, washed and counterstained with DAPI (1:1000 dilution
235 of 5 mg/ml stock, 6335.1, Carl Roth GmbH) to visualize nuclei. Tissues were mounted on glass slides in
236 Dabco-Mowiol 4-88 (Sigma-Aldrich Cat# D2522 and Cat# 81381).
237
238 **Image acquisition and processing**
239 Confocal images and stacks were acquired with Olympus FV1000 confocal microscope equipped with 20X
240 UPlan S-Apo (NA 0.85), 40X UPlan FL (NA 1.30) and 60X UPlanApo (NA1.35) objectives. Maximum Z-
241 projections were generated from consecutive sections taken at 1.4 µm steps using Fluoview 1000
242 Software (Olympus) (RRID: SCR_014215) and Fiji (https://fiji.sc/) (RRID:SCR_002285). Final image
243 processing, including panel assembly, brightness and contrast adjustments were performed in Adobe
244 Photoshop CC (Adobe Systems, Inc.) (RRID:SCR_014199).
245
246 **Quantification of mCherry, RNase H1::GFP, and SmD3::3xHA signal**
247 Fluorescent signal intensity was quantified with Fiji (https://fiji.sc/) (RRID:SCR_002285). For mCherry and
248 RNase H1::GFP, a square selection was created in the middle of the pouch region, and the „Mean
249 intensity" was measured, then the same selection was moved to the middle of the notum and the
250 measurement was repeated. The two values were divided to produce a pouch/notum intensity ratio for
251 each wing disc. For SmD3::3xHA, the „Mean intensities" of SmD3::3xHA and mRFP signals in the pouch
252 region were measured and divided to produce a normalized value for each wing disc. Zoom images of the
253 nubbin domain of independent WDs were used to count the number of SmD3::3xHA-positive punctae per

254 1000 μm^2 area. Statistical significance was determined by one-way ANOVA with Tukey's multiple
255 comparison test (signal intensity) or Kruskall-Wallis test (puncta) in GraphPad Prism (RRID:SCR_002798).
256
257
258 **ACKNOWLEDGEMENTS**

259 We thank Norbert Perrimon for discussions and comments on the manuscript. We thank the Bloomington
260 *Drosophila* Stock Center (BDSC, Bloomington, IN, USA), the Vienna *Drosophila* Resource Center (VDRC,
261 Vienna, Austria), *Drosophila* Genomic Resource Center (DGRC, supported by NIH grant 2P40OD010949,
262 Bloomington, IN, USA), the Zurich ORFeome Project (FlyORF, Zurich, Switzerland) for fly stocks and
263 plasmids. We are grateful to Tina Bresser for generation of transgenic lines and Nils Teuscher for fly stock
264 maintenance and technical assistance.
265
266
267 **REFERENCES**

268 Aughey GN, Grice SJ, Liu J-L (2016) The Interplay between Myc and CTP Synthase in Drosophila. *PLOS*
269 *Genetics* 12: e1005867

270 Bao S, Cagan R (2006) Fast cloning inverted repeats for RNA interference. *RNA* 12: 2020-2024

271 Bischof J, Sheils EM, Björklund M, Basler K (2014) Generation of a transgenic ORFeome library in
272 Drosophila. *Nature protocols* 9: 1607-1620

273 Blake AJ, Finger DS, Hardy VL, Ables ET (2017) RNAi-Based Techniques for the Analysis of Gene Function
274 in Drosophila Germline Stem Cells. *Methods in molecular biology (Clifton, NJ)* 1622: 161-184

275 Brand AH, Perrimon N (1993) Targeted gene expression as a means of altering cell fates and generating
276 dominant phenotypes. *Development* 118: 401-415

277 Crossley MP, Bocek M, Cimprich KA (2019) R-Loops as Cellular Regulators and Genomic Threats. *Mol Cell*
278 73: 398-411

279 Dietzl G, Chen D, Schnorrer F, Su KC, Barinova Y, Fellner M, Gasser B, Kinsey K, Oppel S, Scheiblauer S *et*
280 *al* (2007) A genome-wide transgenic RNAi library for conditional gene inactivation in Drosophila. *Nature*
281 448: 151-156

282 Echeverri CJ, Beachy PA, Baum B, Boutros M, Buchholz F, Chanda SK, Downward J, Ellenberg J, Fraser
283 AG, Hacohen N *et al* (2006) Minimizing the risk of reporting false positives in large-scale RNAi screens.
284 *Nature Methods* 3: 777-779

285 Erkelenz S, Stanković D, Mundorf J, Bresser T, Claudius A-K, Boehm V, Gehring NH, Uhlirova M (2021)
286 Ecd promotes U5 snRNP maturation and Prp8 stability. *Nucleic Acids Research*

287 Giordano E, Rendina R, Peluso I, Furia M (2002) RNAi triggered by symmetrically transcribed transgenes
288 in Drosophila melanogaster. *Genetics* 160: 637-648

289 Graca FA, Sheffield N, Puppa M, Finkelstein D, Hunt LC, Demontis F (2021) A large-scale transgenic RNAi
290 screen identifies transcription factors that modulate myofiber size in Drosophila. *PLOS Genetics* 17:
291 e1009926

292 Green EW, Fedele G, Giorgini F, Kyriacou CP (2014) A Drosophila RNAi collection is subject to dominant
293 phenotypic effects. *Nat Methods* 11: 222-223

294 Hagan CE, Warren GJ (1983) Viability of palindromic DNA is restored by deletions occurring at low but
295 variable frequency in plasmids of Escherichia coli. *Gene* 24: 317-326

296 Hu Y, Comjean A, Roesel C, Vinayagam A, Flockhart I, Zirin J, Perkins L, Perrimon N, Mohr SE (2017)
297 FlyRNAi.org-the database of the Drosophila RNAi screening center and transgenic RNAi project: 2017
298 update. *Nucleic Acids Res* 45: D672-D678

299 Kaya-Çopur A, Schnorrer F (2016) A Guide to Genome-Wide In Vivo RNAi Applications in Drosophila.
300 *Methods Mol Biol* 1478: 117-143

301 Kennerdell JR, Carthew RW (1998) Use of dsRNA-mediated genetic interference to demonstrate that
302 frizzled and frizzled 2 act in the wingless pathway. *Cell* 95: 1017-1026

303 Kim-Yip RP, Nystul TG (2018) Wingless promotes EGFR signaling in follicle stem cells to maintain self-
304 renewal. *Development* 145: dev168716

305 Ledru M, Clark CA, Brown J, Verghese S, Ferrara S, Goodspeed A, Su TT (2022) Differential gene
306 expression analysis identified determinants of cell fate plasticity during radiation-induced regeneration
307 in Drosophila. *PLoS Genet* 18: e1009989

308 Lee YS, Carthew RW (2003) Making a better RNAi vector for Drosophila: use of intron spacers. *Methods*
309 30: 322-329

310 Lesch C, Jo J, Wu Y, Fish GS, Galko MJ (2010) A targeted UAS-RNAi screen in Drosophila larvae identifies
311 wound closure genes regulating distinct cellular processes. *Genetics* 186: 943-957

312 Lohmann JU, Endl I, Bosch TC (1999) Silencing of developmental genes in Hydra. *Dev Biol* 214: 211-214

313 Neely GG, Kuba K, Cammarato A, Isobe K, Amann S, Zhang L, Murata M, Elmen L, Gupta V, Arora S *et al*
314 (2010) A global in vivo Drosophila RNAi screen identifies NOT3 as a conserved regulator of heart
315 function. *Cell* 141: 142-153

316 Ni JQ, Liu LP, Binari R, Hardy R, Shim HS, Cavallaro A, Booker M, Pfeiffer BD, Markstein M, Wang H *et al*
317 (2009) A Drosophila resource of transgenic RNAi lines for neurogenetics. *Genetics* 182: 1089-1100

318 Ni JQ, Markstein M, Binari R, Pfeiffer B, Liu LP, Villalta C, Booker M, Perkins L, Perrimon N (2008) Vector
319 and parameters for targeted transgenic RNA interference in Drosophila melanogaster. *Nat Methods* 5:
320 49-51

321 Perkins LA, Holderbaum L, Tao R, Hu Y, Sopko R, McCall K, Yang-Zhou D, Flockhart I, Binari R, Shim HS *et*
322 *al* (2015) The Transgenic RNAi Project at Harvard Medical School: Resources and Validation. *Genetics*
323 201: 843-852

324 Perrimon N, Ni JQ, Perkins L (2010) In vivo RNAi: today and tomorrow. *Cold Spring Harb Perspect Biol* 2:
325 a003640

326 Piccin A, Salameh A, Benna C, Sandrelli F, Mazzotta G, Zordan M, Rosato E, Kyriacou CP, Costa R (2001)
327 Efficient and heritable functional knock-out of an adult phenotype in Drosophila using a GAL4-driven
328 hairpin RNA incorporating a heterologous spacer. *Nucleic Acids Research* 29

329 Pletcher RC, Hardman SL, Intagliata SF, Lawson RL, Page A, Tennessen JM (2019) A Genetic Screen Using
330 the Drosophila melanogaster TRiP RNAi Collection To Identify Metabolic Enzymes Required for Eye
331 Development. *G3 (Bethesda)* 9: 2061-2070

332 Port F, Hausmann G, Basler K (2011) A genome-wide RNA interference screen uncovers two p24 proteins
333 as regulators of Wingless secretion. *EMBO Rep* 12: 1144-1152

334 Reece-Hoyes JS, Walhout AJM (2018) Gateway Recombinational Cloning. *Cold Spring Harb Protoc* 2018:
335 pdb.top094912

336 Rotelli MD, Bolling AM, Killion AW, Weinberg AJ, Dixon MJ, Calvi BR (2019) An RNAi Screen for Genes
337 Required for Growth of Drosophila Wing Tissue. *G3 Genes|Genomes|Genetics* 9: 3087-3100

338 Rubin GM, Spradling AC (1982) Genetic transformation of Drosophila with transposable element vectors.
339 *Science* 218: 348-353

340 Rust K, Tiwari MD, Mishra VK, Grawe F, Wodarz A (2018) Myc and the Tip60 chromatin remodeling
341 complex control neuroblast maintenance and polarity in Drosophila. *EMBO J* 37

342 Rylee J, Mahato S, Aldrich J, Bergh E, Sizemore B, Feder LE, Grega S, Helms K, Maar M, Britt SG *et al*
343 (2022) A TRiP RNAi screen to identify molecules necessary for Drosophila photoreceptor differentiation.
344 *G3 Genes|Genomes|Genetics*: jkac257

345 Saj A, Arziman Z, Stempfle D, van Belle W, Sauder U, Horn T, Dürrenberger M, Paro R, Boutros M,
346 Merdes G (2010) A Combined Ex Vivo and In Vivo RNAi Screen for Notch Regulators in Drosophila
347 Reveals an Extensive Notch Interaction Network. *Developmental Cell* 18: 862-876

348 Santos-Pereira JM, Aguilera A (2015) R loops: new modulators of genome dynamics and function. *Nat*
349 *Rev Genet* 16: 583-597

350 Sarov M, Schneider S, Pozniakovski A, Roguev A, Ernst S, Zhang Y, Hyman AA, Stewart AF (2006) A
351 recombineering pipeline for functional genomics applied to Caenorhabditis elegans. *Nat Methods* 3:
352 839-844

353 Tomari Y, Zamore PD (2005) Perspective: machines for RNAi. *Genes Dev* 19: 517-529

354 van der Graaf K, Srivastav S, Singh P, McNew JA, Stern M (2022) The Drosophila attP40 docking site and
355 derivatives are insertion mutations of MSP300. *bioRxiv*: 2022.2005.2014.491875

356 Vissers JH, Manning SA, Kulkarni A, Harvey KF (2016) A Drosophila RNAi library modulates Hippo
357 pathway-dependent tissue growth. *Nat Commun* 7: 10368

358 Wargelius A, Ellingsen S, Fjose A (1999) Double-stranded RNA induces specific developmental defects in
359 zebrafish embryos. *Biochem Biophys Res Commun* 263: 156-161

360 Wianny F, Zernicka-Goetz M (2000) Specific interference with gene function by double-stranded RNA in
361 early mouse development. *Nat Cell Biol* 2: 70-75

362 Zamore PD, Tuschl T, Sharp PA, Bartel DP (2000) RNAi: double-stranded RNA directs the ATP-dependent
363 cleavage of mRNA at 21 to 23 nucleotide intervals. *Cell* 101: 25-33

364 Zeng X, Han L, Singh SR, Liu H, Neumuller RA, Yan D, Hu Y, Liu Y, Liu W, Lin X *et al* (2015) Genome-wide
365 RNAi screen identifies networks involved in intestinal stem cell regulation in Drosophila. *Cell Rep* 10:
366 1226-1238

367 Zhou J, Xu L, Duan X, Liu W, Zhao X, Wang X, Shang W, Fang X, Yang H, Jia L *et al* (2019) Large-scale RNAi
368 screen identified Dhpr as a regulator of mitochondrial morphology and tissue homeostasis. *Science*
369 *Advances* 5: eaax0365

370 Zielke N, Korzelius J, van Straaten M, Bender K, Schuhknecht GFP, Dutta D, Xiang J, Edgar BA (2014) Fly-
371 FUCCI: A versatile tool for studying cell proliferation in complex tissues. *Cell Rep* 7: 588-598
372

373

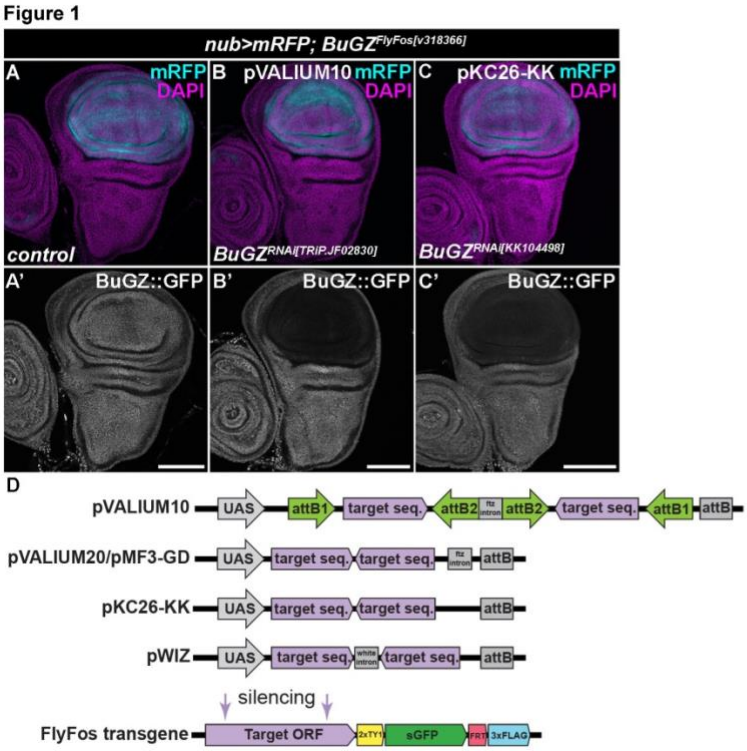

Figure 1. pVALIUM10 and KK RNAi lines cause efficient silencing.

(A-C) Expression of pVALIUM10 *BuGZ*$^{RNAi[TRIP.JF02830]}$ (B, B') and KK-based *BuGZ*$^{RNAi[KK104498]}$ transgenic RNAi lines (C, C') using the *nubbin-Gal4, UAS-myr-mRFP* driver (*nub>mRFP*, light blue) causes a marked reduction of a BuGZ$^{FlyFos[v318366]}$ transgenic protein in the pouch region of wing discs (WDs) relative to the hinge and notum, and control WD (A, A'). Micrographs show projections of multiple confocal sections of WDs dissected from third instar larvae 7 days AEL. The multiple-tagged BuGZ$^{FlyFos\ [v318366]}$ protein was visualized by immunostaining with an anti-GFP antibody (white). Nuclei were counterstained with DAPI (magenta). Scale bars: 100 μm. **(D)** Schematic representation of various vectors used for cloning and overexpression of dsRNA. In the absence of the target-specific antibody, the RNAi efficacy can be assessed with the help of FlyFos transgenes expressing multiple-tagged proteins under the control of the endogenous regulatory sequences.

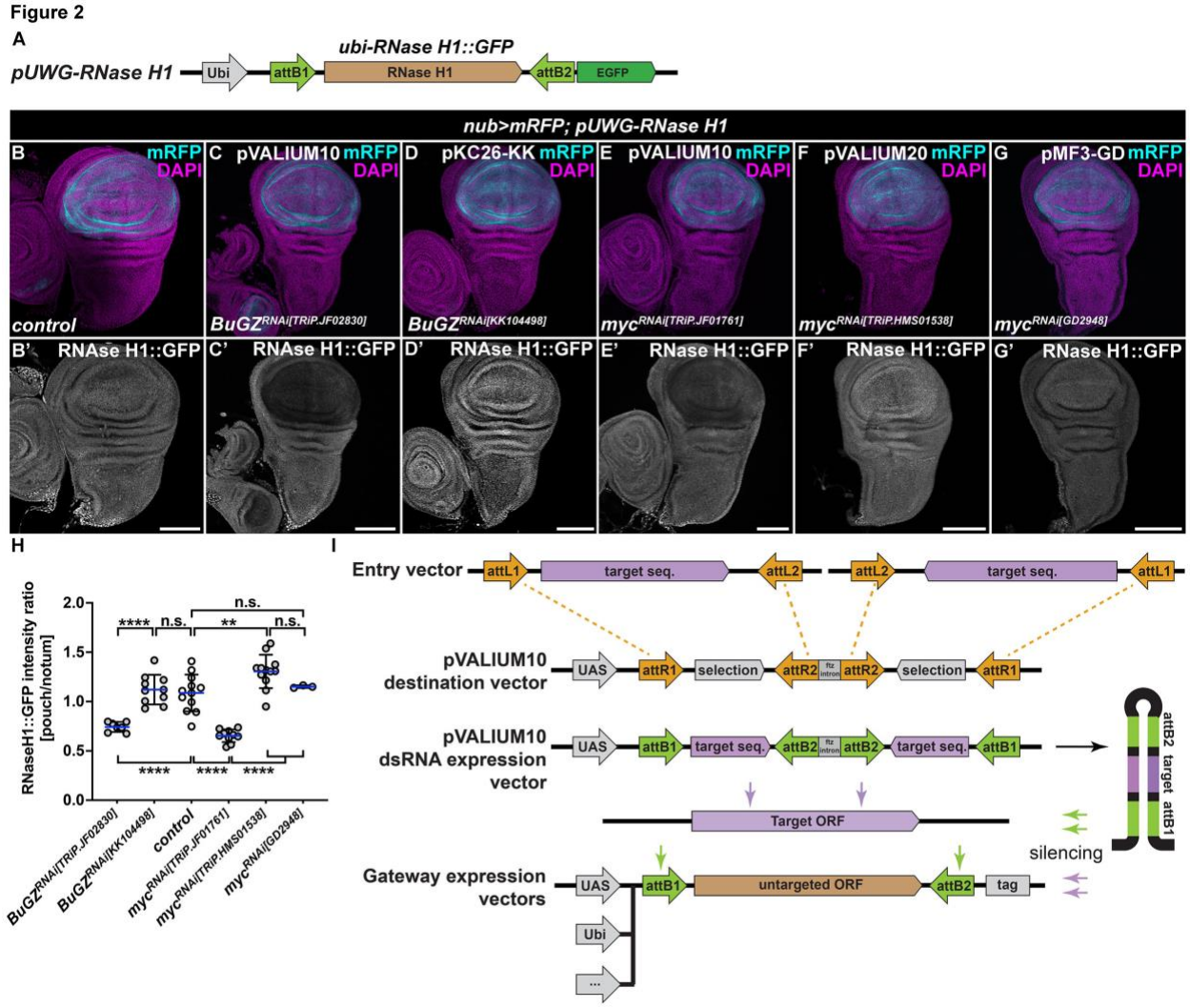

387

388 **Figure 2. pVALIUM10-based lines cause off-target silencing of the RNAse H1::GFP transgenic reporter.**

389 **(A)** Schematic representation of the transgenic *pUWG-RNase H1* reporter construct expressing the C-

390 terminally-tagged RNase H1::GFP protein from the ubiquitous (*ubi*) promoter. The *RNase H1* coding

391 sequence is flanked by attB1 and attB2 sites generated via Gateway-mediated recombination catalyzed

392 by the LR clonase. **(B-G)** Immunostaining with a GFP-specific antibody revealed a marked reduction of the

393 RNase H1::GFP levels in the nubbin domain (mRFP, light blue), where pVALIUM10-based

394 *BuGZ*$^{RNAi[TRIP.JF02830]}$ (C) and *myc*$^{RNAi[TRiP.JF01761]}$ (E) RNAi lines were expressed using the *nubbin-Gal4, UAS-myr-*

395 *mRFP* driver (*nub>mRFP*). No such downregulation of the RNase H1::GFP signal was observed in control

396 WD (B) and following expression of KK-based *BuGZ*$^{RNAi[KK104498]}$ (D), pVALIUM20-based *myc*$^{RNAi[TRiP.HMS01538]}$

397 (F) or GD-based *myc*$^{RNAi[GD2948]}$ (G). Micrographs show projections of multiple confocal sections of WDs
398 dissected from third instar larvae 7 days AEL. Nuclei were counterstained with DAPI (magenta). Scale bars:
399 100 μm. **(H)** Quantification of the RNase H1::GFP signal depicted as relative intensity ratio between the
400 pouch and notum region. Statistical significance was determined by one-way ANOVA with Tukey's
401 multiple comparison test; n ≥ 3; **p<0.01, ****p<0.0001, n.s. non-significant. **(I)** Generation of
402 pVALIUM10 RNAi lines relied on a LR clonase-mediated recombination of dsRNA fragment from an Entry
403 vector to the pVALIUM10 destination vector (Ni *et al.,* 2009). The dsRNA hairpin produced from the
404 pVALIUM10 dsRNA expression vector is the source of siRNA species targeting the transcript of interest
405 (target ORF) but also attB1 and attB2 sites present in any of the Gateway expression vectors generated
406 via the same recombination mechanisms.
407

Figure 3

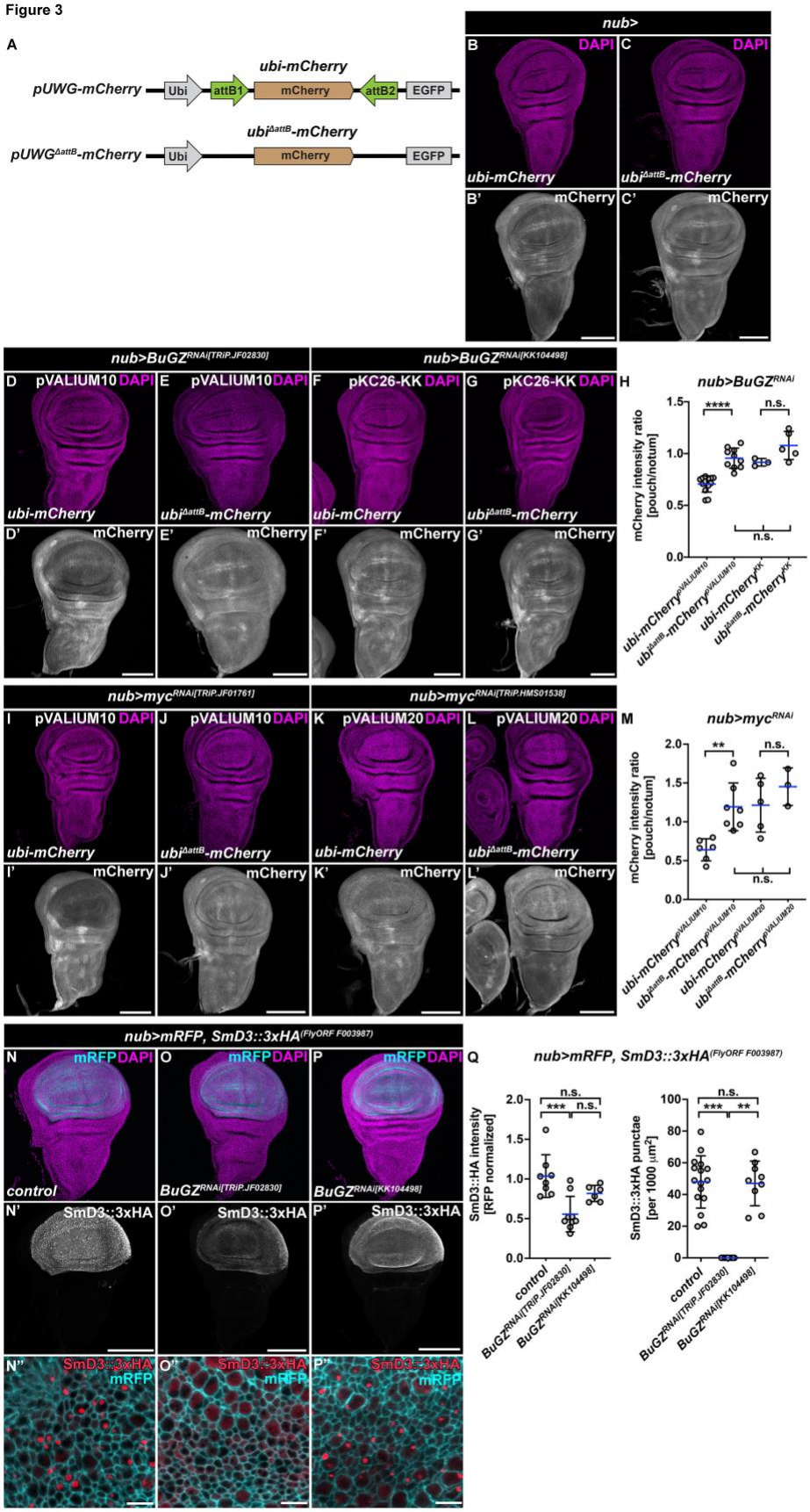
A
pUWG-mCherry
Ubi
attB1
ubi-mCherry
mCherry
attB2
EGFP
pUWGΔattB-mCherry
ubiΔattB-mCherry
nub>
B
DAPI
C
ubi-mCherry
ubiΔattB-mCherry
B'
mCherry
C'
nub>BuGZRNAi[TRiP.JF02830]
nub>BuGZRNAi[KK104498]
D
pVALIUM10
E
pKC26-KK
F
G
D'
E'
F'
G'
H
nub>BuGZRNAi
mCherry intensity ratio [pouch/notum]
****
n.s.
ubi-mCherryVALIUM10
ubiΔattB-mCherryVALIUM10
ubi-mCherryKK
ubiΔattB-mCherryKK
nub>mycRNAi[TRiP.JF01761]
nub>mycRNAi[TRiP.HMS01538]
I
J
K
pVALIUM20
L
I'
J'
K'
L'
M
nub>mycRNAi
**
ubi-mCherryVALIUM20
ubiΔattB-mCherryVALIUM20
nub>mRFP, SmD3::3xHA(FlyORF F003987)
N
mRFP
O
P
control
BuGZRNAi[TRiP.JF02830]
BuGZRNAi[KK104498]
N'
SmD3::3xHA
O'
P'
N''
SmD3::3xHA
mRFP
O''
P''
Q
SmD3::HA intensity [RFP normalized]
***
SmD3::3xHA punctae [per 1000 μm²]
control
BuGZRNAi[TRiP.JF02830]
BuGZRNAi[KK104498]

408

409 **Figure 3. pVALIUM10 RNAi lines silence Gateway transgenes via attB1 and attB2 sites.**

410 **(A)** Schematic of the transgenic *pUWG-mCherry* and mutant *pUWG*$^{\Delta attB}$*-mCherry* reporter constructs. The
411 mCherry is expressed from the poly-ubiquitin (*ubi*) promoter. **(B, C)** *ubi-mCherry* and mutant *ubi*$^{\Delta attB}$-
412 *mCherry* reporters showed similar expression pattern in the wing imaginal discs. **(D-M)** *ubi-mCherry* was
413 efficiently downregulated by pVALIUM10 *BuGZ*$^{RNAi[TRIP.JF02830]}$ and *myc*$^{RNAi[TRiP.JF01761]}$ expressed under the
414 control of the *nubbin-Gal4* driver (*nub>*) relative to the rest of the WD (D, I, H, M). In contrast, absence of
415 attB1 and attB2 sequences rendered the *ubi*$^{\Delta attB}$*-mCherry* reporter resistant to pVALIUM10 RNAi-mediated
416 silencing (E, H, J, M). Neither KK- (*BuGZ*$^{RNAi[KK104498]}$) nor pVALIUM20-based (*myc*$^{RNAi[TRiP.HMS01538]}$) RNAi lines
417 affected mCherry levels expressed from the unmodified or mutant reporter constructs (F-H, K-M).
418 Micrographs show projections of multiple confocal sections of WDs dissected from third instar larvae 7
419 days AEL that were immunostained with an anti-mRFP antibody (white). Nuclei were counterstained with
420 DAPI (magenta). Scale bars: 100 μm. Quantification of mCherry signal depicted as relative intensity ratio
421 between the pouch and notum region (H, M). Superscript text in each group denotes the type of RNAi
422 used. Statistical significance was determined by one-way ANOVA with Tukey's multiple comparison test;
423 $n \geq 3$; **$p<0.01$, ****$p<0.0001$, n.s. non-significant. **(N-Q)** Expression of pVALIUM10 *BuGZ*$^{RNAi[TRIP.JF02830]}$
424 (O) in the wing pouch using *nubbin-Gal4, UAS-mRFP* driver (*nub>mRFP*) reduces SmD3::3xHA levels
425 compared to control (N) and KK-based *BuGZ*$^{RNAi[KK104498]}$ (P). Note foci of SmD3::3xHA protein in control
426 (N") and *BuGZ*$^{RNAi[KK104498]}$ cells (P") cells that are not present in *BuGZ*$^{RNAi[TRIP.JF02830]}$ expressing cells (O").
427 Micrographs show projections of multiple or single (N"-P") confocal sections of WDs dissected from third
428 instar larvae 7 days AEL that were immunostained with an anti-HA antibody (white, N'-P'; red, N"-P").
429 Nuclei were counterstained with DAPI (magenta). Scale bars: 100 μm or 5 μm (N"-P"). Quantification of
430 the SmD3::3xHA signal intensity (Q, left) and SmD3::3xHA-positive punctae (Q, right) in the pouch region.
431 Statistical significance was determined by one-way ANOVA with Tukey's multiple comparison test and
432 Kruskall-Wallis test, respectively; $n \geq 6$; **$p<0.01$, ***$p<0.001$, n.s. non-significant.